Analytical Methods

Accepted Manuscript

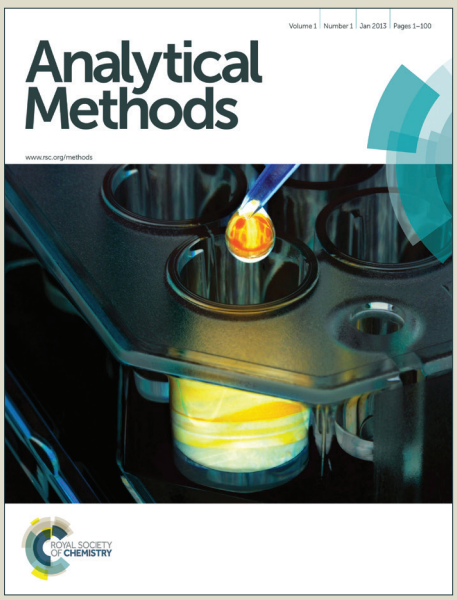

ROYAL SOCIETY OF CHEMISTRY

www.rsc.org/methods

Graphical Abstract

Label-free DNA detection based on oligonucleotide-stabilized silver nanoclusters and exonuclease III-catalyzed target recycling amplification

Hui Ma, Wei Wei, Qian Lu, Zhixin Zhou, Henan Li, Linqun Zhang and Songqin Liu*

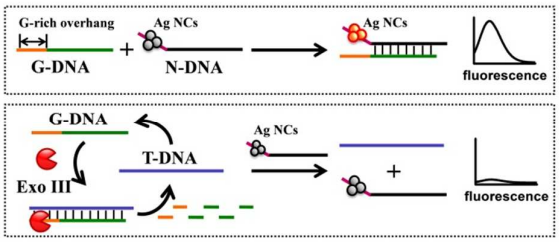

A label-free DNA biosensor with high sensitivity and selectivity is constructed by DNA-Ag NCs and Exo III-catalyzed target recycling amplification.

Cite this: DOI: 10.1039/c0xx00000x

www.rsc.org/xxxxxx

ARTICLE TYPE

Label-free DNA detection based on oligonucleotide-stabilized silver nanoclusters and exonuclease III-catalyzed target recycling amplification

Hui Ma, Wei Wei, Qian Lu, Zhixin Zhou, Henan Li, Linqun Zhang and Songqin Liu*

Received (in XXX, XXX) Xth XXXXXXXXX 20XX, Accepted Xth XXXXXXXXX 20XX
DOI: 10.1039/b000000x

As an emerging class of metal nanoclusters, oligonucleotide-stabilized silver nanoclusters (DNA-Ag NCs) show a number of applications in biosensing and bionanotechnology. Herein, we develop a label-free DNA sensor based on DNA-Ag NCs and exonuclease III (Exo III)-catalyzed target recycling amplification. The fluorescence of single-strand DNA-stabilized Ag NCs can be enhanced through hybridization with the guanine-rich DNA. With the addition of target DNA, the fluorescence intensity decreases comparable with that of DNA duplex-stabilized Ag NCs, which is attributed to the competitive hybridization reaction. With the help of Exo III, the fluorescence intensity decreases more obviously. The calibration range for target DNA is 0.3 to 30 nM, and the detection limit is 0.2 nM. The sensor offers 100-fold improvement in detection sensitivity compared with that obtained without Exo III. The proposed strategy also shows excellent selectivity, which can differentiate between perfectly matched and mismatched target DNA. Therefore, the strategy presents a promising platform for DNA detection with high sensitivity and selectivity.

Introduction

Noble metal nanoclusters, comprising of several to hundreds of atoms, have gained much attention owing to their unique fluorescence properties and potential applications in biosensor and bionanotechnology.[1-6] Among these noble metal clusters, silver nanoclusters (Ag NCs) possess good solubility, excellent photophysical properties and low toxicity, which makes them become promising substitutes for organic dyes and quantum dots for the aforementioned applications.[5-10] More strikingly, oligonucleotide-stabilized silver nanoclusters (DNA-Ag NCs) exhibit outstanding features, such as their facile synthesis, tunable fluorescence emission and high photostability.[11-17] The fluorescence emission spectra of DNA-Ag NCs are highly DNA-sequence-dependent, which can be tuned throughout visible and near IR region just by changing the sequence and length of oligonucleotides.[15-17] Besides, the fluorescence intensity of DNA-Ag NCs can be enhanced by 500-fold when they are in close proximity to guanine-rich (G-rich) DNA sequences.[18] Moreover, DNA-Ag NCs have been successfully applied to cell imaging,[19,20] metal ions detection,[21,22] protein assay[23,24] and DNA sensing.[25-28] However, the challenge of how to achieve lower detection limit with the novel nanomaterial has not been well addressed, particularly for DNA assays.[26-30]

The sensitive DNA detection is of vital importance for mutation identification, gene therapy and monitoring of hybridization reaction.[31-33] Recently, the strategies based on enzyme-catalyzed signal amplification have been performed via polymerase,[34,35] nicking endonuclease[36,37] and exonuclease[38-41] for sensitive DNA detection. Among them, exonuclease III (Exo III) is a kind of exonuclease that can selectively catalyze the stepwise removal of mononucleotides from blunt or recessed 3′ termini of double-stranded DNA.[40,41] Compared with nicking endonuclease,[36,37] Exo III does not require specific recognition sequences, which makes it become an ideal candidate for constructing a universal signal amplification platform. The method based on Exo III-catalyzed signal amplification has been carried out to obtain sensitive DNA detection in combination with graphene oxide or gold nanoparticles.[42,43] Recently, our group has developed a biosensor for colorimetric DNA detection based on gold nanoparticles and Exo III. The sensor offers the detection sensitivity as low as 2 nM and good selectivity with naked eyes.[43]

Herein, we report a sensitive, selective, and label-free strategy for DNA detection based on DNA-Ag NCs and Exo III-catalyzed target recycling amplification. As shown in Scheme 1A, N-DNA has an Ag NCs-nucleation sequence. The single-strand DNA-stabilized Ag NCs are synthesized with N-DNA and exhibit almost no fluorescence. Upon addition of G rich-DNA (G-DNA) to the solution of N-DNA-stabilized Ag NCs (N-DNA-Ag NCs), the G-rich overhang gets close proximity to the prepared N-DNA-Ag NCs through hybridization, and the fluorescence intensity increases dramatically.[18] When a low concentration of target DNA (T-DNA) is added to the mixture of N-DNA-Ag NCs and G-DNA, more stable T/G-DNA duplex can be formed. And the fluorescence intensity decreases due to the decrease in the amount of N/G-DNA duplex-stabilized Ag NCs (N/G-DNA-Ag

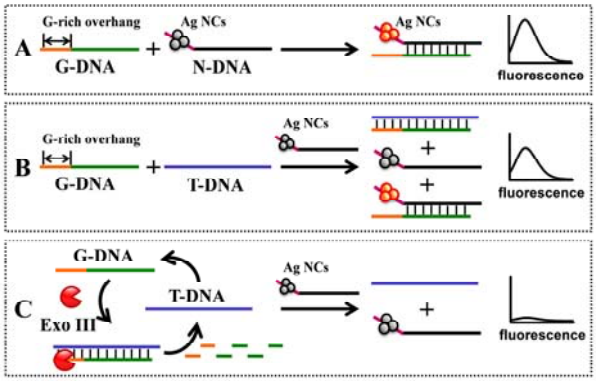

Scheme 1 (A) Schematic illustration of the fluorescence enhancement of DNA-Ag NCs caused by the proximity of G-rich overhang. (B) Schematic representation of DNA detection just based on DNA-Ag NCs. (C) Schematic representation of amplified DNA detection based on DNA-Ag NCs and Exo III.

NCs) (Scheme 1B). With the simultaneous addition of Exo III and T-DNA to the mixture of N-DNA-Ag NCs and G-DNA, the fluorescence intensity decreases more obviously because of Exo III amplification (Scheme 1C). Based on these results, the sensor with Exo III amplification allows the detection of T-DNA with a detection limit of 0.2 nM, which is much lower than the detection limits of previously reported DNA-Ag NCs-based sensors without enzymatic amplification (12.5 nM,[30] 14 nM[28] and 200 nM[29]). Moreover, this strategy can effectively distinguish perfectly matched from mismatched target DNA. Therefore, the method represents good application prospect for DNA detection.

Experimental

Reagents

All oligonucleotides were purchased from Sangon Biotechnology Co., Ltd (Shanghai, China). All sequences of the oligonucleotides used in the assay were listed in Table S1 (ESI†). The oligonucleotides were stored in phosphate buffer solution (20 mM phosphate, 1 mM magnesium acetate, pH 7.4). Exonuclease III (Exo III) was obtained from TAKARA biotechnology Co., Ltd. (Dalian, China) and used without additional purification. Silver nitrate ($AgNO_3$) and sodium borohydride ($NaBH_4$) were obtained from Sinopharm Chemical Reagent Co., Ltd. (Nanjing, China). Other chemicals were of analytical grade. All aqueous solutions were prepared with double distilled water.

Apparatus

UV-vis absorption spectra were recorded with a UV-visible spectrometer (Shimadzu UV-2450, Japan), and fluorescence measurements were performed on FluoroMax-4 spectro-fluorometer (Horiba, Japan). The morphologies of Ag NCs were observed with transmission electron microscopy (TEM, JEM-2010, Japan). CD spectra of DNA were collected by a Chirascan Circular Dichroism (Applied Photophysics, UK), and the optical chamber (0.1 cm path length) was kept under a stable stream of dry purified nitrogen (99.99%) during experiments.

Synthesis of N-DNA-Ag NCs

N-DNA-Ag NCs were synthesized according to the previous literature with minor modification.[15,24] Briefly, N-DNA (4 μM) and 24 μM $AgNO_3$ were sequentially mixed with 20 mM phosphate buffer (1.0 mM Mg^{2+}, pH 7.4). After cooling on the ice for 15 min, 24 μM $NaBH_4$ aqueous solution (freshly prepared) was added quickly, followed by vigorous shaking for 1 min. The reduction time of the mixture in the dark at 4 °C was at least 3h (ESI, Fig. S1†). The prepared N-DNA-Ag NCs solution was stored in the dark at 4 °C prior to use.

DNA detection

In a typical hybridization assay, 0.5 μM G-DNA, 15 U Exo III and various concentrations of target DNA were incubated at 37 °C for 2 h. The mixture was heated at 80 °C for 20 min to deactivate Exo III and then slowly cooled to room temperature. Afterwards, 0.5 μM N-DNA-Ag NCs solution was added to the above solution. The mixture was incubated at 37 °C for 1 h (ESI, Fig. S2†). The concentration of target DNA was detected by measuring the fluorescence decrease compared with the fluorescence intensity of N/G-DNA-Ag NCs.

Results and discussion

Characterization of DNA-Ag NCs

The formation of DNA-Ag NCs could be characterized by the transmission electron microscope (TEM). As shown in Fig. 1A, DNA-Ag NCs were monodispersed with an average size of approximately 2 nm. Fig. 1B showed that N/G-DNA-Ag NCs exhibited strong fluorescence emission at 623 nm with excitation at 564 nm. The characteristic absorption peak was observed in the UV-vis spectra, which had a maximum wavelength that was identical to that of the fluorescence excitation peak (ESI, Fig. S5†, curve b). The N/G-DNA-Ag NCs displayed pale pink color under room light and bright red color under UV lamp irradiations (Inset in Fig. 1B). The room temperature quantum yield of the N/G-DNA-Ag NCs was calculated to be about 15% against the reference of Rhodamine B in water (ESI, Fig. S3†), which was comparable with the reported results.[20,21,44] Furthermore, N-DNA-Ag NCs and N/G-DNA-Ag NCs were stable upto one week in the dark at 4 °C (ESI, Fig. S4†).

Verification of the assay principle

The principle of the assay was shown in Scheme 1. In our assay, N-DNA involved an Ag NCs-nucleation sequence (pink color), a hybridization sequence and an adenine-rich sequence (black color). G-DNA involved a sequence that was complementary to N-DNA (green color) and a G-rich sequence (orange color).

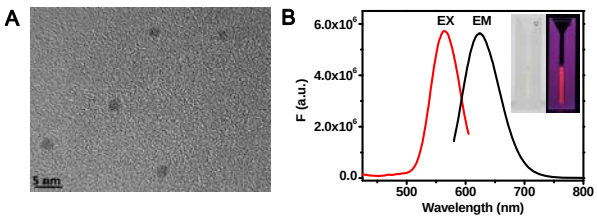

Fig. 1 (A) TEM image of DNA-Ag NCs. (B) Excitation (λ_{ex} = 564 nm) and emission (λ_{em} = 623 nm) spectra of N/G-DNA-Ag NCs. Inset: Photographs of the fluorescent Ag NCs solution under (left) room light and (right) UV lamp irradiations. [N-DNA] = 10 μM, [G-DNA] = 10 μM.

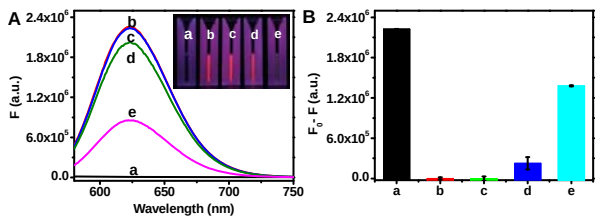

Fig. 2 (A) Fluorescence spectra and (B) Fluorescence decrease of solutions (a) N-DNA-Ag NCs, (b) N/G-DNA-Ag NCs, (c) N/G-DNA-Ag NCs in the presence of Exo III, (d) N/G-DNA-Ag NCs in the presence of T-DNA, (e) N/G-DNA-Ag NCs in the presence of T-DNA and Exo III. Inset in A: Photographs of the above Ag NCs solutions under UV lamp irradiations. [N-DNA] = 500 nM, [G-DNA] = 500 nM, [T-DNA] = 50 nM, [Exo III] = 15 U; [N-DNA] = 10 μM, [G-DNA] = 10 μM, [T-DNA] = 1 μM, [Exo III] = 300 U in (Inset).

Scheme 1A illustrated that the fluorescence enhancement of DNA-Ag NCs caused by the proximity of G-rich overhang. N-DNA-Ag NCs exhibited weak fluorescence (Fig. 2A, curve a). After adding G-DNA to the solution of N-DNA-Ag NCs, N/G-DNA-Ag NCs were formed. And the fluorescence intensity could be dramatically enhanced (Fig. 2A, curve b), which was attributed to the fact that the hybridization between G-DNA and N-DNA brought the G-rich overhang close to the prepared Ag NCs. The DNA detection just based on the DNA-Ag NCs was represented in Scheme 1B. Compared with N-DNA, T-DNA had 18 longer complementary bases hybridized with G-DNA. When the longer bases compared to N-DNA were less than 7, the rate of strand displacement reaction was low.[45] Meanwhile, N-DNA in N/G-DNA-Ag NCs was hard to be displaced by T-DNA because the affinity between T-DNA and G-DNA was not enough strong. When the longer bases compared to N-DNA were more than 20, secondary structure tended to form,[46] and the hybridization efficiency between T-DNA and G-DNA decreased. This result has also been verified by our group.[43] In the assay, the presence of T-DNA prevented G-DNA from hybridizing with N-DNA, which resulted in the decrease in the amount of N/G-DNA-Ag NCs. Upon the addition of T-DNA to the mixture of N-DNA-Ag NCs and G-DNA, the fluorescence intensity slightly decreased because of the competitive hybridization reaction (Fig. 2A, curve d). As shown in Scheme 1C, with the simultaneous addition of T-DNA and Exo III to the mixture of N-DNA-Ag NCs and G-DNA, T/G-DNA duplex with a blunt end at the 3′ terminus was formed. G-DNA in this kind of DNA duplex could be digested by Exo III, and then T-DNA was released from the T/G-DNA duplex.[40,41] The released T-DNA hybridized with another G-DNA to induce a new cleavage reaction, which resulted in the digestion of a large amount of G-DNA. Thus, a remarkable decrease in the fluorescence intensity was observed (Fig. 2A, curve e). On the other hand, with the addition of Exo III to the mixture of N-DNA-Ag NCs and G-DNA, the fluorescence change was almost not observed (Fig. 2A, curve c). The results proved that N/G-DNA duplex was not digested by Exo III. The corresponding photograph under UV lamp irradiations for the above Ag NCs solutions was shown in the inset of Fig. 2A. The solution with Exo III amplification could be discerned easily with naked eyes. Furthermore, the fluorescence decrease displayed 6-fold enhancement after Exo III was added to the mixture of N-DNA-Ag NCs, G-DNA and T-DNA (Fig. 2B), confirming the successful Exo III-catalyzed target recycling amplification.

The circular dichroism (CD) spectra were also used to verify the principle of the designed strategy (Fig. 3). CD spectra showed significant enhancement of peak intensity and a shift of peak position from 251 nm to 248 nm before (curve a) and after (curve b) hybridization of N-DNA-Ag NCs with G-DNA. With the addition Exo III to the mixture of N-DNA-Ag NCs and G-DNA, the ellipticity at 248 nm had almost no change compared with N/G-DNA-Ag NCs (curve c). In the presence of a low concentration of T-DNA, the peak intensity at 248 nm became a little stronger (curve d). The reason was that the formation of T/G-DNA duplex led to the decrease in the amount of N/G-DNA-Ag NCs. Therefore, the ellipticity of the former was stronger than that of the latter. This was in accordance with the reported results that the ellipticity of the DNA-Ag NCs was weaker than that of free DNA due to the formation of folded DNA structure.[11,47] In the presence of Exo III and T-DNA simultaneously, an obvious decrease of peak intensity and a shift of peak position from 248 nm to 249 nm were observed (curve e), which was close to the spectra of N-DNA-Ag NCs. This proved that a number of N-DNA-Ag NCs existed in the solution, which was attributed to the fact that a number of G-DNA was digested by Exo III. Besides, Exo III amplification could be further verified by the corresponding UV-vis absorption spectra, which were recorded in Fig. S5 (ESI†). All of the above results demonstrated the successful Exo III-catalyzed target recycling amplification.

Optimization of assay conditions

The ratio of G-DNA to N-DNA-Ag NCs (G/N ratio) would affect the sensitivity for DNA detection. As shown in Fig. 4, the fluorescence intensity increased with the increasing G/N ratio and reached a maximum value at the G/N ratio of 1.5 (curve a). However, the increase of G/N ratio led to the rapid decrease of signal to background (S/B) ratio ($(F_0\text{-}F)/F_0$) from 0.94 to 0.05 (curve b). F_0 corresponded to the fluorescence intensity of N/G-DNA-Ag NCs, and (F_0-F) corresponded to the fluorescence decrease of the solution comparable with N/G-DNA-Ag NCs.

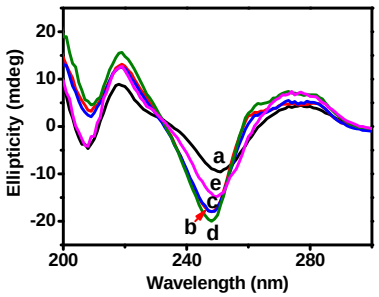

Fig. 3 CD spectra of solutions (a) N-DNA-Ag NCs, (b) N/G-DNA-Ag NCs, (c) N/G-DNA-Ag NCs in the presence of Exo III, (d) N/G-DNA-Ag NCs in the presence of T-DNA, (e) N/G-DNA-Ag NCs in the presence of T-DNA and Exo III. [N-DNA] = 10 μM, [G-DNA] = 10 μM, [T-DNA] = 1 μM, [Exo III] = 300 U.

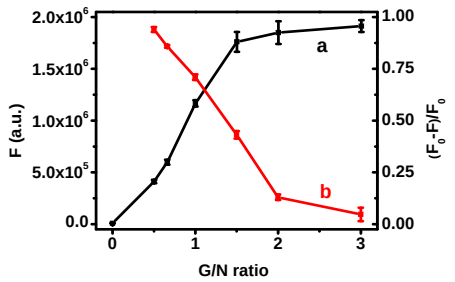

Fig. 4 Effect of the ratio of G-DNA to N-DNA-Ag NCs (G/N ratio) on (a) the signal (F) and (b) signal to noise ratio (F_0-F)/F_0. Error bars are calculated based on three replicates. [N-DNA] = 500 nM, [T-DNA] = 100 nM.

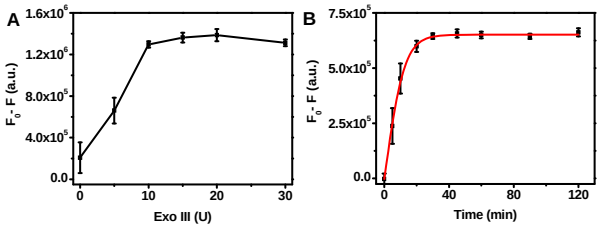

Fig. 5 Effect of (A) the amount of Exo III and (B) the digestion time of Exo III on the fluorescence decrease of the assay. Error bars are calculated based on three replicates. [N-DNA] = 500 nM, [G-DNA] = 500 nM, [T-DNA] = 50 nM, [Exo III] = 15 U.

The S/B ratio reduced to as low as 0.43 at the G/N ratio of 1.5. Considering from the detection sensitivity, the ratio of 1 (S/B = 0.71) was selected as the optimal G/N ratio.

The enzymatic reaction condition was also vital to the assay. Fig. 5A showed that the fluorescence decrease increased significantly with increasing amount of Exo III and was nearly saturated at 15 U. The amount was close to the reported result, in which the sensor exhibited high detection sensitivity and good double-stranded selectivity by using 16 U Exo III.[42] The Exo III-catalyzed target recycling reaction was rapid, and the fluorescence decrease reached a platform after 30 min in the presence of 15 U Exo III (Fig. 5B). In order to obtain complete cleavage effect of Exo III, 2 hours were chosen as incubation time in the whole assay.

Sensitivity and selectivity of the sensor

Under the optimal assay condition, the fluorescence intensity gradually decreased with increasing concentration of T-DNA either in the absence or presence of Exo III. In the absence of Exo III, the fluorescence decrease was linear with the concentration of T-DNA in the range of 30-200 nM with a correlation coefficient of 0.997, and the detection limit was 20 nM in terms of 3 times deviation of blank sample. In the presence of Exo III, the fluorescence decrease was linear with the concentration of T-DNA in the range of 0.3-30 nM with a correlation coefficient of 0.999 (Fig. 6). The detection limit was reduced to 0.2 nM, which was much lower than that of other biosensors based on DNA-Ag NCs (12.5 nM-200 nM).[28-30] Moreover, the sensor assisted with Exo III had about 100-fold improvement in the sensitivity with respect to that without Exo III.

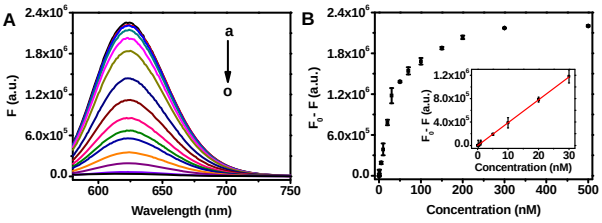

Fig. 6 (A) Fluorescence spectra of N/G-DNA-Ag NCs in the presence of Exo III and various concentrations of T-DNA. T-DNA concentrations from (a) to (o) are 0, 0.3, 0.5, 1, 5, 10, 20, 30, 50, 70, 100, 150, 200, 300 and 500 nM. (B) Fluorescence decrease changed with the increasing concentration of T-DNA. Inset showes the linear relationship between the fluorescence decrease and the concentration of T-DNA (R=0.999). Error bars are calculated based on three replicates. [N-DNA] = 500 nM, [G-DNA] = 500 nM, [Exo III] = 15 U.

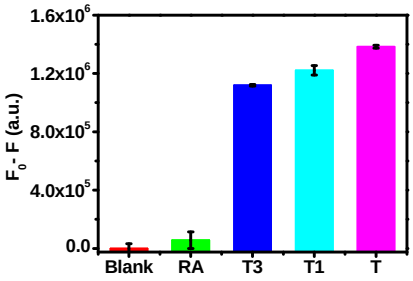

Fig. 7 Histogram of the selectivity of the assay. N/G-DNA-Ag NCs (Blank), N/G-DNA-Ag NCs in the presence of random target DNA (RA), three-base mismatched target DNA (T3), one-base mismatched target DNA (T1), perfectly matched target DNA (T). Error bars are calculated based on three replicates. [N-DNA] = 500 nM, [G-DNA] = 500 nM, [T-DNA] = 50 nM, [Exo III] = 15 U.

To investigate the selectivity of the strategy, we recorded the fluorescence decrease of N/G-DNA-Ag NCs (Blank) in the presence of perfect matched target DNA (T), one-base mismatched target DNA (T1), three-base mismatched target DNA (T3) and random target DNA (RA). As shown in Fig. 7, the presence of perfectly matched target DNA in N/G-DNA-Ag NCs led to the obvious fluorescence decrease, while no fluorescence decrease was observed by adding random target DNA. Due to the impaired hybridization efficiency of mismatched DNA duplex and the special digestion function of Exo III, the fluorescence decrease became smaller as the number of mismatched bases increased. Therefore, the results exhibited that perfectly matched target DNA could be distinguished from mismatched target DNA and random target DNA, suggesting the high specificity of the proposed sensor for DNA detection.

Conclusions

In this work, a label-free DNA biosensor based on DNA-Ag NCs and Exo III-catalyzed target recycling amplification has been constructed. With the help of Exo III, the detection limit is as low as 0.2 nM, and the sensor has 100-fold improvement in sensitivity with respect to that without Exo III. Using DNA-Ag NCs as fluorescent probes and G-rich DNA as signal enhancers, the strategy needs no separation procedures, complex labeling processes and sophisticated instruments. Besides, the strategy shows high selectivity toward target DNA and provides a

technique for discriminating perfectly matched target DNA from mismatched target DNA. Thus, this innovative strategy presents a promising platform for sensitive and selective detection of DNA.

Acknowledgments

The project is supported by the National Natural Science Foundation of China (Grant No. 21205014), the Natural Science Foundation of Jiangsu province (BK2012734), the Social Development Project of Jiangsu (BE2012731) and the Social Development Project of Suzhou (ZXY2012027).

Notes and references

Key Laboratory of Environmental Medicine Engineering, Ministry of Education, School of Chemistry and Chemical Engineering, Southeast University, Jiangning District, Nanjing, 211189, P.R. China. Fax: 86-25-5209061; Tel.: 86-25-52090613; E-mail addresses: liusq@seu.edu.cn

† Electronic Supplementary Information (ESI) available: [details of any supplementary information available should be included here]. See DOI: 10.1039/b000000x/

1 J. P. Wilcoxon and B. L. Abrams, Chem. Soc. Rev., 2006, **35**, 1162-1194.
2 J. Zheng, P. R. Nicowich and R. M. Dickson, Annu. Rev. Phys. Chem., 2007, **58**, 409-431.
3 Y. L. Wang, J. J. Chen and J. Irudayaraj, ACS Nano, 2011, **5**, 9718-9725.
4 F. Samari, B. Hemmateenejad, Z. Rezaei and M. Shamsipur, Anal. Methods, 2012, **4**, 4155–4160.
5 L. A. Peyser, A. E. Vinson, A. P. Bartko and R. M. Dickson, Science, 2001, **291**, 103-106.
6 H. Xu and K. S. Suslick, Adv. Mater., 2010, **22**, 1078-1082.
7 N. de Souza, Nat. Methods, 2007, **4**, 540-540.
8 J. Zhang, S. Xu and E. Kumacheva, Adv. Mater., 2005, **17**, 2336-2340.
9 M. Kuno, D. P. Fromm, H. F. Hamann, A. Gallagher and D. J. Nesbitt, J. Chem. Phys., 2000, **112**, 3117-3120.
10 S. F. Lee and M. A. Osborne, J. Am. Chem. Soc., 2007, **129**, 8936-8937.
11 J. T. Petty, J. Zheng, N. V. Hud and R. M. Dickson, J. Am. Chem. Soc., 2004, **126**, 5207-5212.
12 T. Vosch, Y. Antoku, J. C. Hsiang, C. I. Richards, J. I. Gonzalez and R. M. Dickson, Proc. Natl. Acad. Sci. U.S.A., 2007, **104**, 12616-12621.
13 B. Sengupta, C. M. Richie, J. G. Buckman, K. R. Johnsen, P. T. Goodwin and J. T. Petty, J. Phys. Chem. C, 2008, **112**, 18776-18782.
14 S. Choi, R. M. Dickson and J. Yu, Chem. Soc. Rev., 2012, **41**, 1867-1891.
15 C. I. Richards, S. Choi, J. C. Hsiang, Y. Antoku, T. Vosch, A. Bongiorno, Y. L. Tzeng and R. M. Dickson, J. Am. Chem. Soc., 2008, **130**, 5038-5039.
16 E. G. Gwinn, P. O'Neill, A. J. Guerrero, D. Bouwmeester and D. K. Fygenson, Adv. Mater., 2008, **20**, 279-283.
17 J. Sharma, H. C. Yeh, H. Yoo, J. H. Werner and J. S. Martinez, Chem. Commun., 2010, **46**, 3280-3282.
18 H. C. Yeh, J. Sharma, J. J. Han, J. S. Martinez and J. H. Werner, Nano Lett., 2010, **10**, 3106-3110.
19 Z. P. Sun, Y. L. Wang, Y. T. Wei, R. Liu, H. R. Zhu, Y. Y. Cui, Y. L. Zhao and X. Y. Gao, Chem. Commun., 2011, **47**, 11960-11962.
20 Y. W. Zhou, C. M. Li, Y. Liu and C. Z. Huang, Analyst, 2013, **138**, 873–878.
21 G. Y. Lan, C. C. Huang and H. T. Chang, Chem. Commun., 2010, **46**, 1257-1259.
22 G. L. Liu, D. Q. Feng, T. F. Chen, D. Li and W. J. Zheng, J. Mater. Chem., 2012, **22**, 20885-20888.
23 J. Sharma, H. C. Yeh, H. Yoo, J. H. Werner and J. S. Martinez, Chem. Commun., 2011, **47**, 2294-2296.
24 J. J. Li, X. Q. Zhong, H. Q. Zhang, X. C. Le and J. J. Zhu, Anal. Chem., 2012, **84**, 5170-5174.
25 W. W. Guo, J. P. Yuan, Q. Z. Dong and E. K. Wang, J. Am. Chem. Soc., 2010, **132**, 932-934.
26 J. T. Petty, B. Sengupta, S. P. Story and N. N. Degtyareva, Anal. Chem., 2011, **83**, 5957-5964.
27 J. T. Petty, S. P. Story, S. Juarez, S. S. Votto, A. G. Herbst, N. N. Degtyareva and B. Sengupta, Anal. Chem., 2012, **84**, 356-364.
28 G. Y. Lan, W. Y. Chen and H. T. Chang, Biosens. Bioelectron., 2011, **26**, 2431-2435.
29 Z. X. Zhou, Y. Du and S. J. Dong, Biosens. Bioelectron., 2011, **28**, 33-37.
30 J. P. Yuan, W. W. Guo and E. K. Wang, Anal. Chim. Acta, 2011, **706**, 338-342.
31 J. G. Hacia, L. C. Brody, M. S. Chee and S. P. Fodor, Nat. Genet, 1996, **14**, 441-447.
32 J. B. Fan, M. S. Chee and K. L. Gunderson, Nat. Rev. Genet., 2006, **7**, 632-644.
33 Y. J. Zhao, X. W. Zhao, B. C. Tang, W. Y. Xu, J. Li, J. Hu and Z. Z. Gu, Adv. Funct. Mater., 2010, **20**, 976-982.
34 Q. Guo, X. Yang, K. Wang, W. Tan, W. Li, H. Tang and H. Li, Nucleic Acids Res., 2009, **37**, e20.
35 A. R. Connolly and M. Trau, Angew. Chem. Int. Ed., 2010, **49**, 2720-2723.
36 J. J. Li, Y. Chu, B. Y. H. Lee and X. S. Xie, Nucleic Acids Res., 2008, **36**, e36.
37 W. Xu, X. Xue, T. Li, H. Zeng and X. Liu, Angew. Chem. Int. Ed., 2009, **48**, 6849-6852.
38 J. A. Dougan, D. MacRae, D. Graham and K. Faulds, Chem. Commun., 2011, **47**, 4649-4651.
39 X. L. Zuo, F. Xia, Y. Xiao and K. W. Plaxco, J. Am. Chem. Soc., 2010, **132**, 1816-1818.
40 C. C. Richardson, I. R. Lehman and A. J. Kornberg, Biol. Chem., 1964, **239**, 251-258.
41 H. J. Lee, Y. Li, A. W. Wark and R. M. Corn, Anal. Chem., 2005, **77**, 5096-5100.
42 P. Hu, C. Z. Zhu, L. H. Jin and S. J. Dong, Biosens. Bioelectron., 2012, **34**, 83-87.
43 Z. X. Zhou, W. Wei, Y. J. Zhang and S. Q. Liu, J. Mater. Chem. B, 2013, **1**, 2851-2858.
44 J. H. Shen, Y. H. Zhu, C. Chen, X. L. Yang and C. Z. Li, Chem. Commun., 2011, **47**, 2580-2582.
45 Q. G. Li, G. Y. Luan, Q. P. Guo and J. X. Liang, Nucleic Acids Res., 2002, **30**, e5.
46 B. D. Smith, N. Dave, P. J. Huang and J. Liu, J. Phys. Chem. C, 2011, **115**, 7851-7857.
47 G. Y. Lan, W. Y. Chen and H. T. Chang, Biosens. Bioelectron., 2011, **26**, 2431-2435.